This is an open access article published under an ACS AuthorChoice License, which permits copying and redistribution of the article or any adaptations for non-commercial purposes.

ACS OMEGA

Article

http://pubs.acs.org/journal/acsodf

Light-Assisted Solvothermal Chemistry Using Plasmonic Nanoparticles

Hadrien M. L. Robert,*[,†,‡] Franziska Kundrat,[¶] Esteban Bermúdez-Ureña,[§] Hervé Rigneault,[†] Serge Monneret,[†] Romain Quidant,[§,∥] Julien Polleux,[¶,#] and Guillaume Baffou*[,†]

[†]Institut Fresnel, CNRS, Aix-Marseille Université, Centrale Marseille, UMR 7249, 13013 Marseille, France

[‡]PHASICS S.A., Parc technologique de Saint Aubin, Route de l'Orme des Merisiers, 91190 Saint Aubin, France

[¶]Department of Molecular Medicine, Max Planck Institute of Biochemistry, 82152 Martinsried, München, Germany

[§]ICFO - Institut de Ciències Fotòniques, The Barcelona Institute of Science and Technology, 08860 Castelldefels, Barcelona, Spain

[∥]ICREA - Institució Catalana de Recerca i Estudis Avançats, 08010 Barcelona, Spain

[#]Center for NanoScience, Ludwig Maximilian University, 80799 Munich, Germany

ABSTRACT: Solvothermal synthesis, denoting chemical reactions occurring in metastable liquids above their boiling point, normally requires the use of a sealed autoclave under pressure to prevent the solvent from boiling. This work introduces an experimental approach that enables solvothermal synthesis at ambient pressure in an open reaction medium. The approach is based on the use of gold nanoparticles deposited on a glass substrate and acting as photothermal sources. To illustrate the approach, the selected hydrothermal reaction involves the formation of indium hydroxide microcrystals favored at 200 °C in liquid water. In addition to demonstrating the principle, the benefits and the specific characteristics of such an approach are investigated, in particular, the much faster reaction rate, the achievable spatial and time scales, the effect of microscale temperature gradients, the effect of the size of the heated area, and the effect of thermal-induced microscale fluid convection. This technique is general and could be used to spatially control the deposition of virtually any material for which a solvothermal synthesis exists.

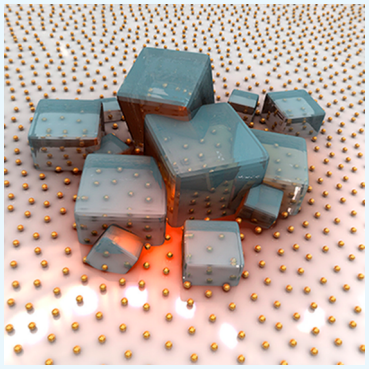

INTRODUCTION

Plasmon-induced nanochemistry (PINC) is an active area of research that benefits from the plasmonic properties of metal nanoparticles to enhance or enable chemical reactions on small scales.[1] Three main features of plasmonic nanoparticles have been involved so far in PINC: (1) the enhanced optical near field of nanoparticles,[2−4] which favors photochemical reactions in the vicinity of the illuminated particles, (2) heat generation,[5−10] which favors local chemical synthesis according to the Arrhenius law, and (3) hot electron/hole injection,[11−13] a recently proposed mechanism leading to localized redox reactions. These multiple facets of plasmonic nanoparticles provide a wide variety of tools to develop new applications in nanochemistry. The aim of this work is to introduce a novel approach in PINC based on the use of plasmonic nanoparticles as nanosources of heat, enabling solvothermal reactions.

Solvothermal chemical synthesis relies on the use of superheated liquid solvents, that is, liquids heated above their boiling point. For water, it typically corresponds to temperature ranging from 100 to 380 °C. To prevent the solvent from boiling and to keep it a liquid at such high temperatures, the standard procedure involves the use of a sealed chamber, named an *autoclave*, in which the temperature increase concomitantly creates a pressure increase that maintains the solvent in a liquid state.

The interest of a solvothermal (or hydrothermal) synthesis is manifold. For instance, many organic compounds that are inert in liquid water become reactive when the temperature is increased far above 100 °C, especially reactions that occur only in the presence of strong acid or base. Indeed, as temperature increases from 20 to 300 °C, the ionic product of water increases by three orders of magnitude, from $10^{-14.0}$ to $10^{-11.3}$. The resulting higher concentrations of OH^- and H_3O^+ simultaneously increase the rate of both acid- and base-catalyzed reactions in liquid water far beyond the natural acceleration thermally governed by the Arrhenius law. Moreover, the dielectric constant of water decreases from 80.1 down to 19.7 over this range of temperature, which results in a strong decrease of the polarity of water molecules and in a natural rise of solubility of ionic compounds. Today, the growing interest in using hydrothermal synthesis derives from its advantages in terms of high reactivity of reactants, formation of a metastable and unique solvent, and low energy consumption.[14] The main constraint of such an approach relies on the use of an autoclave, which prevents any chemical exchange and monitoring during the reaction.

Received: April 20, 2016
Accepted: May 6, 2016
Published: July 6, 2016

 © 2016 American Chemical Society

DOI: 10.1021/acsomega.6b00019
ACS Omega 2016, 1, 2−8

In this article, we show that solvothermal synthesis can be achieved under ambient conditions without requiring a pressure chamber when heating is performed by illuminating a substrate patterned with metal nanoparticles illuminated at their plasmonic resonance. Such experimental conditions prevent the liquid from boiling, up to around 220 °C, as recently evidenced in a previous work.[15] We illustrate this approach with a well-established solvothermal chemical reaction involving the synthesis of indium hydroxide microcrystals in water. After describing the experimental conditions and the results, we dedicate a final part to discuss the interest, the benefits and the limitations of plasmon-assisted solvothermal chemistry (PASC).

RESULTS

Liquid Superheating Using Metal Nanoparticles. Under illumination at their plasmonic resonance wavelength, metal nanoparticles can turn into efficient heat sources. This effect is the basis of an active field of research named thermoplasmonics,[16] involving promising biomedical applications. We have recently shown that, against all odds, water superheating can be achieved at ambient pressure by heating plasmonic nanoparticles on a glass substrate using continuous wave (cw) laser illumination.[15] The geometry of the system is depicted in Figures 1 and 2. The sample was composed of a glass coverslip patterned with (1) a uniform distribution of gold nanorings made by block copolymer micellar lithography (BCML)[17] (see Figure 1a) or (2) isolated gold disks, 500 nm in diameter and 40 nm thick, made by e-beam lithography (EBL) (not shown).

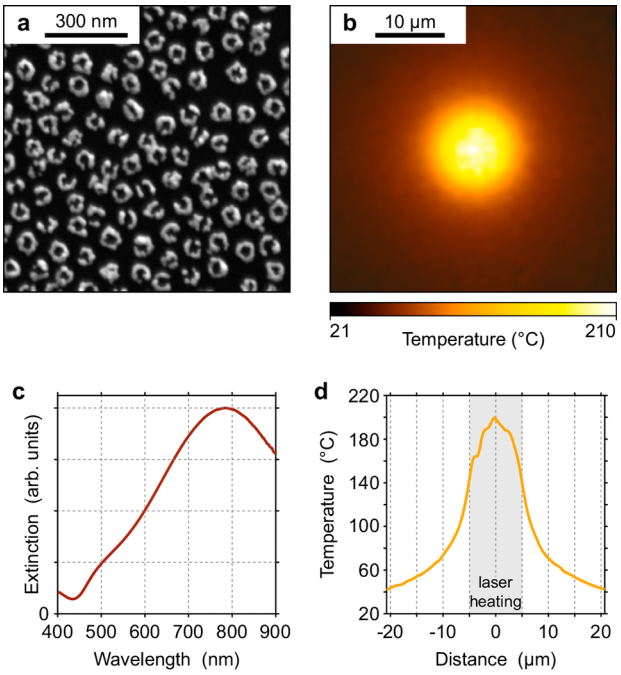

Figure 1. (a) Gold nanorings on a glass substrate made by BCML. (b) Associated temperature distribution (155 × 155 px) when the sample is illuminated with a laser beam, 10 μm in diameter, reaching a value close to 200 °C at the center of the heated area. (c) Extinction spectrum of the BCML substrate made of gold nanorings in water. (d) Temperature profile related to image (b) averaged over 11 successive horizontal lines across the center of the image.

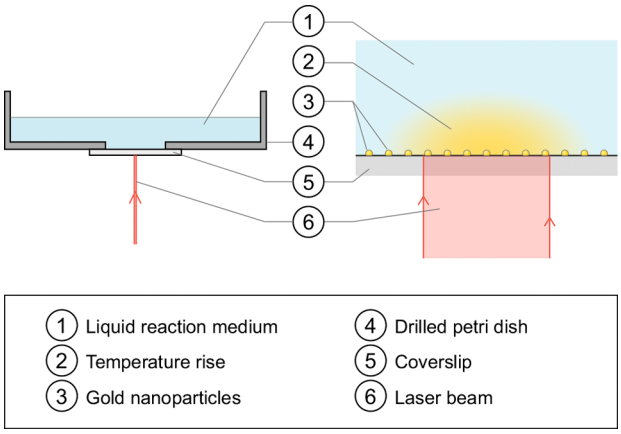

Figure 2. Side view of the sample where the hydrothermal synthesis takes place.

The coverslip was pasted on the back of a drilled Petri dish, which was filled with the reactants freshly dissolved in deionized (Milli-Q) water (Figure 2). The sample was finally placed on an optical microscope enabling optical (intensity and phase) imaging, laser heating and temperature imaging at the submicrometric scale (see ref 18 for details). Heating was performed by illuminating the sample from below (i.e., from the glass side) using a laser beam at λ = 800 nm, matching the plasmonic resonance wavelength of the gold nanoparticles. When working with BCML samples, the beam profile at the glass/water interface was expanded to obtain a uniform (not Gaussian) beam with a diameter that could be adjusted from a few microns to a few hundreds of microns using an iris (see Figure 1b). When working with EBL samples, the laser beam was rather focused on a single gold disk using a 100× objective, NA 1.3. In any configuration, water superheating was systematically observed but we have never seen water boiling at 100 °C. Bubble formation systematically occurred around 220 ± 10 °C, as evidenced experimentally by the thermal microscopy technique we developed (Figure 1b).[18]

The reason why water does not boil is that this system is free from nucleation points, such as scratches, micrometric cavities, impurities, and so on. Glass surfaces are particularly flat by nature, and it turns out that gold nanoparticles do not act as nucleation point themselves.[15]

Hydrothermal Synthesis. Hydrothermal synthesis refers to solvothermal synthesis where the solvent is water. To simply evidence that solvothermal synthesis can be conducted at ambient pressure using gold nanoparticles, we selected a hydrothermal chemical reaction[19] that involves the formation of solid particles, namely, the chemical transformation of indium chloride to indium hydroxide crystals

$$InCl_{3(aq)} + 3OH^- \xrightarrow{200\ °C} In(OH)_{3(s)} + 3Cl^-$$

Typical crystals obtained with this approach feature a cubic crystallographic symmetry, as evidenced in ref 19.

We initially prepared a solution under the same experimental conditions as in ref 19. We dissolved 0.21 g of $InCl_3$, 9.4 mg of NaOH, and 12.5 μL of NH_3 in 24 mL of water, which gave a concentration of c_m = 40 mM $InCl_3$. This solution was then diluted 10, 100, or 1000 times before being added into the Petri dish. Prior to each experiment, calibration was made using our thermal microscopy technique with pure water in the sample to determine which laser power was required to reach 200 °C for a

DOI: 10.1021/acsomega.6b00019
ACS Omega 2016, 1, 2−8

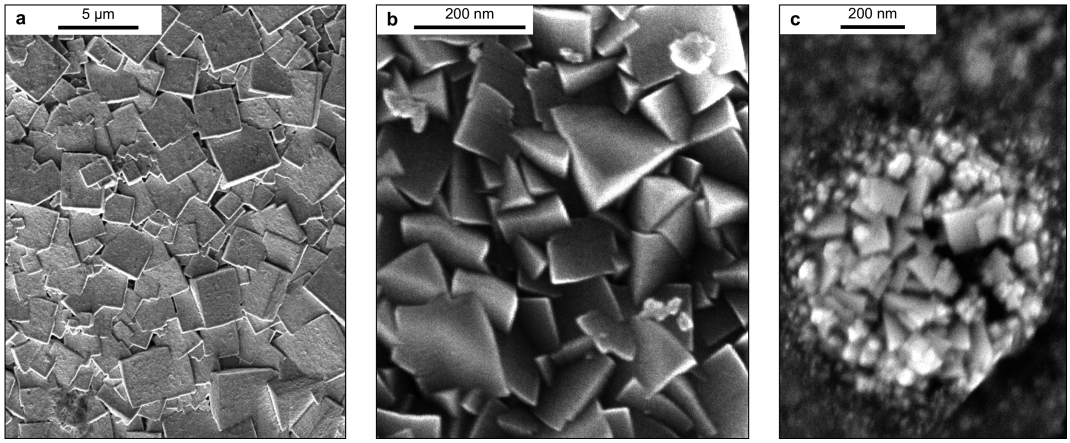

Figure 3. Effect of the size of the heated area. (a) SEM image of $In(OH)_3$ microcrystals formed upon heating an area of 500 μm in diameter (BCML sample, laser exposure time δt = 1 h, laser power = 380 mW, maximum temperature T_0 = 200 °C, and reactant concentration c_m = 40 mM). (b) SEM image of $In(OH)_3$ microcrystals formed upon heating an area of 10 μm in diameter (BCML sample, laser exposure time δt = 1 h, laser power = 18.5 mW, maximum temperature T_0 = 200 °C, and reactant concentration $c_0 = c_m/10$ = 4 mM). (c) SEM image of $In(OH)_3$ microcrystals formed upon heating a single gold disk, 430 nm in diameter (EBL sample, laser exposure time δt = 10 min, laser power = 0.43 mW, maximum temperature T_0 = 200 °C, and reactant concentration $c_0 = c_m/1000$ = 0.04 mM).

given laser beam size. Note that the use of a thermal microscopy technique is not mandatory; if a setup is not endowed with a means of temperature characterization, it is possible to ensure a temperature of around 200 °C by setting the laser power slightly below the laser power threshold for bubble formation (supposed to be around 230 °C).

In our approach, a set of four parameters can be adjusted, namely, (1) the laser beam diameter D (i.e., the size of the heated area in the case of BCML samples), (2) the temperature T_0 (taken at the center of the heated area), (3) the initial reactant concentration c_0, and (4) the heating duration δt.

Reaction Kinetics. We first conducted experiments upon heating at T_0 = 200 °C an area with a diameter ranging from 430 nm (gold disk) to 500 μm (BCML sample). Figure 3 shows SEM (scanning electron microscopy) images taken at the center of the illuminated area where cubic $In(OH)_3$ crystals have grown. Several important observations can be made.

(1) In comparison with the standard high-pressure procedure, which yields the formation of isolated clusters of particles, the local photothermal approach leads to a dense coverage of the substrate where the crystals can be partially merged with each other. The dimension of the crystals ranged from a few 100 nm to 4 μm, which is comparable with common results obtained with an autoclave.

(2) The smaller the heated area, the faster the reaction rate. For instance, when using a single gold disk, 430 nm in diameter, we observed a fast crystal formation (10 min) although the reactant concentration was divided by a factor of 1000 ($c_0 = c_m/1000$). We interpret this observation by the constant renewal of the reactants in the confined heated volume because of Brownian motion, fluid convection,[20] and thermophoresis.[21−23] Indeed, the micrometric reaction volume is in contact with a quasi infinite reservoir of reactants (the rest of the liquid volume), which maintains the reactant concentration constant during the reaction. Thus, one observed kinetics with an effective 0th order, hence the faster product formation. For further details on the origin of this effect, let us use the following notations

$$[InCl_3] = c(t) \tag{1}$$

$$[In(OH)_3] + [InCl_3] = c_0 \tag{2}$$

For the sake of simplicity, we assume a first-order reaction. In this case, the reaction rate r reads

$$r = \frac{d[In(OH)_3]}{dt} \tag{3}$$

$$= -\frac{d[InCl_3]}{dt} \tag{4}$$

$$= -\frac{dc(t)}{dt} = Kc(t) \tag{5}$$

where K is the rate constant of the reaction. This differential equation yields

$$[InCl_3] = c_0 e^{-Kt} \tag{6}$$

$$[In(OH)_3] = c_0(1 - e^{-Kt}) \tag{7}$$

$$r = c_0 K e^{-Kt} \tag{8}$$

Now, if the heated volume is much smaller than the size of the system, the concentration of $InCl_3$ can be considered as constant because $InCl_3$ molecules are continuously renewed in the heated region by Brownian motion. Equations 3 and 5 yield

$$r = \frac{d[In(OH)_3]}{dt} = Kc(t) \approx Kc_0 \tag{9}$$

and thus

$$[In(OH)_3] = Kc_0 t \tag{10}$$

The concentration of $In(OH)_3$ is thus linearly increasing as a function of time and no longer limited by an exponential saturation, as in eq 7. This mechanism is inherently related to the geometry of the system and can be seen as a natural Ostwald isolation.

DOI: 10.1021/acsomega.6b00019
ACS Omega 2016, 1, 2−8

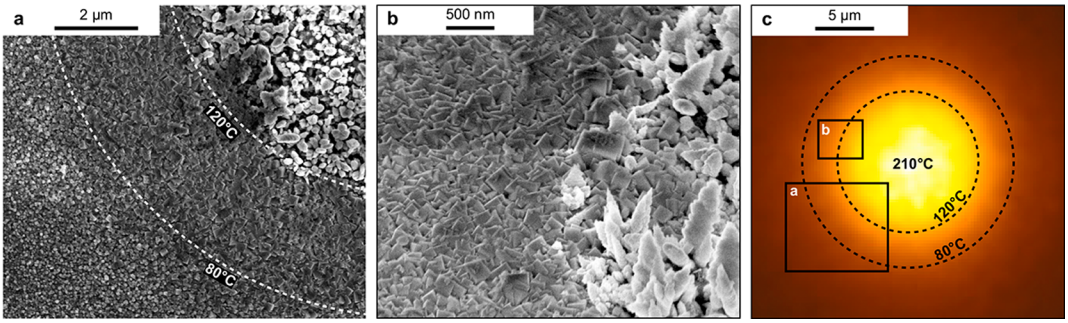

Figure 4. (a) SEM image of crystal formation along a temperature gradient. (b) SEM image highlighting the transition from one type of structure to another. The sample was imaged with a tilt angle of 45°. (c) Measured temperature distribution where the temperature thresholds (dashed lines) and the areas corresponding to the SEM images (a) and (b) (solid lines) have been indicated.

(3) The theory introduced above explains that the larger the system, the slower the reaction rate. It is certainly the reason why kinetics of crystal formation is so long with an autoclave, which usually implies heating duration longer than 20 h. A benefit of our approach is that we can observe the formation of crystals within only a few minutes, with the same reactant concentrations.

(4) Too long an exposure time (or too high a concentration) yields the formation of pine-tree-like structures, another type of structure (Figure 4b). Deviation from regular shapes for too long heating duration was also mentioned in the literature.[24] The reason was related to an Ostwald-ripening mechanism. If heating is carried further on or if we reproduce the exact same conditions of temperature, exposure time, and concentration as with an autoclave, one even observes the formation of a large and smooth dome (hemispherical structure) of the size of the heated area.

(5) It may seem surprising that the crystal products do not act as nucleation points for water boiling once they are formed, even at 200 °C. We have never observed bubble formation because of the formation of nano- and microcrystals. We believe that a nucleation center must consist of a microscale cavity (a scratch) rather than an asperity, a bump, to enable a flat initial curvature radius of a nucleating bubble, that is, a small Laplace overpressure. This is also the reason why the gold nanoparticles themselves do not act as nucleation points; they look like nanoscale bumps rather than microscale cavities.

(6) The heating dynamics can be as fast as the time scale $\tau = L^2/a$, where L is the characteristic size of the heated area and a is the thermal diffusivity of the surrounding medium. For water, $a = 10^{-7}$ $m^2 \cdot s^{-1}$. To give an idea, if the size of the heated area is $L = 10$ μm, the heating time scale can be as fast as 1 ms.

(7) Locally heating a fluid possibly yields fluid convection, even at the micrometric scale and especially when superheating a fluid. If the heated area is less than a micrometer, no strong convection is expected (less than a micrometer per second).[20] However, for a larger heated area, up to 100 μm, substantial convection can be observed (several 10 s of $\mu m \cdot s^{-1}$) and one can wonder what the effect could be on the chemical reaction. Our results show that convection does not affect the crystal growth. It should even favor kinetics by faster renewal of the reactants in the heated region. Furthermore, fluid convection is not supposed to affect the spatial steady-state distribution of temperature because temperature diffusion always occurs faster than thermal-induced fluid convection. This well-known effect in fluid dynamics stems from a large Prandtl number of water ($Pr \approx 7$).[25]

(8) Products remain located at the water/glass interface, where the nanoparticles are located. This may be because, in part, of the fact that it is where the temperature is the largest. However, the surface could also nucleate the formation of crystals by a heterogeneous nucleation process.

Effect of the Temperature Increase. A benefit of using our approach is that any dependence on the temperature increase can be easily studied. One can generate a temperature gradient on a single field-of-view, spanning from 200 °C to ambient temperature, and observe the morphological evolution of the formed crystals along the temperature gradient. Figure 4 presents such a situation. The temperature gradient was measured using our thermal microscopy technique and is displayed in Figure 4c. The resulting crystal formation was imaged using SEM, as presented in Figure 4a,b. We chose a situation where three different domains have been formed. The center domain, where the temperature was close to 200 °C, features the pine-tree-like structures observed when the heating duration is long enough (as mentioned earlier). The intermediate area, ranging from 120 to 80 °C, is covered with the cubic $In(OH)_3$ crystals of interest. Finally, the third zone is not covered with anything crystalline. Interestingly, the transition from one zone to another is extremely well defined and occurs at a precise temperature for a given heating duration. For instance, in the present case (i.e., for a heating duration of 1 h), the transition from pine-tree to cubic shapes occurs at $T = 120$ °C, and cubic crystals do not form below $T = 80$ °C. We used a long exposure time on purpose, to observe three domains. A shorter exposure time would have led to cubic crystals in the center of the heated area and to no pine-tree-like structures.

Noteworthily, in this experiment, one can see that the formation of crystals can be achieved at much lower temperatures than those expected (80−120 °C compared with 200 °C). This observation highlights an additional interest on PASC; because of enhanced kinetics, products can be obtained at reduced temperatures within a reasonable time, even under nonhydrothermal conditions.

DOI: 10.1021/acsomega.6b00019
ACS Omega 2016, 1, 2−8

DISCUSSION

Let us discuss the benefits of plasmon-assisted solvothermal chemistry (PASC) compared with those of using an autoclave at high pressure. (1) PASC yields much faster reactions, as explained above, because of an effective reduction of the order of the reaction by a natural Ostwald flooding. (2) PASC can achieve much faster heating/cooling dynamics, down to the microsecond scale. The temperature quasi-instantaneously rises or drops as soon as the laser illumination is turned on or off because of the weak inertia related to the small volume of the system. (3) PASC enables the observation of product formation using optical means, in real time (with a diffraction-limited resolution, not shown herein). (4) PASC enables the introduction of reactants during the reaction as the reaction medium is not sealed. (5) PASC makes the study of the effect of the temperature increase straightforward. A single experiment reveals the crystal morphologies over a full range of temperatures. (6) An industrial application could be the laser-driven microscale patterning of nano- and microcrystals, using a scanning laser.

It is also worth discussing the benefits of using a layer of gold nanoparticles (as the one displayed in Figure 1a), compared with those of using a uniform absorbing layer (like a metal layer for instance).[26] The real interest does not rely on the fact that plasmonic nanoparticles are much more absorbent. A substrate can be made nearly 100% absorbent without requiring plasmonic nanoparticles, and nanoparticles will never do better than 100% absorption. Also, even if the absorption is not large, the laser power can still be increased to reach the desired temperature. The benefits of using nanoparticles are the following. (1) The heated area can be much smaller than the size of a focused laser beam, down to the size of a single nanoparticle. (2) Metal films are highly reflective. With metal nanoparticles, it is possible to make the light−sample interaction purely absorbent (no scattering, no reflection, only absorption). (3) Depositing a metal layer requires bulky and expensive apparatus, whereas metal nanoparticle substrates (such as BCML samples) can be obtained using chemical means and cheap bench-top devices. (4) Plasmonic nanoparticles exhibit an absorption resonance in a finite region of the spectrum, which makes it possible to heat the sample at a given wavelength range, whereas the sample will remain transparent at other wavelengths. This will make, for instance, observation easier using optical microscopy techniques in the visible range upon heating in the IR range.

Let us now discuss the limitations of our technique. (1) It is not meant to produce large amounts of products (for industrial or commercial purposes for instance). It is rather intended to help fundamental research on solvothermal synthesis or to yield applications in local patterning of microstructures. (2) It is mainly of interest for solid-state products. If the products remain as dissolved species, the interest of PASC is not evident as the products will escape from the heated area because of Brownian motion. However, the production of solid products remains a major aspect of solvothermal synthesis, with a myriad of applications, from the synthesis of microporous crystals, ionic conductors, complex oxides and fluorides, low-dimensional aluminophosphates, inorganic−organic hybrid materials, and particularly condensed materials such as diamond and inorganic helical chains.[14]

Let us finally place the concept of PASC in the context of the state-of-the-art related to light-induced chemistry at the micrometric scale.

The concept of photothermal-induced growth of nano- and microstructures on plasmonic nanoparticles was pioneered by Boyd and coworkers in 2006[27] and then further investigated by other groups.[28−30] The concept introduced by Boyd consisted of a new chemical vapor deposition (CVD) process in which local heating necessary to induce the chemical deposition from a gas phase was performed by local laser heating at the micrometric scale of gold nanoparticles deposited on a substrate. The authors named this technique PACVD (plasmon-assisted CVD). They demonstrated microscale patterning of metal oxides such as PbO and TiO_2 on a glass substrate by local heating up to 150 °C. Their approach was, however, based on a gas environment, not involving a liquid environment in a superheated state, like in our study.

In 2009, Adleman and coworkers introduced the concept of plasmon-assisted catalysis (PAC) in a liquid environment. The authors chose to investigate the thermal-induced reforming of a liquid mixture of ethanol and water, leading to the formation of CO_2, CO, and H_2, favored by the natural catalytic effect of gold nanoparticles.[31,32] The experiments were conducted in a microfluidic channel to ease the collection of the gas products. However, no fluid superheating was involved in the mechanism.

In 2013, Yeo and coworkers[26] reported on the photothermal-induced growth of ZnO nanowires on a metal film acting as a light-absorbing layer. This seminal article is closely related to our work as the authors managed to grow microcrystals at the microscale using a photo-hydrothermal effect. However, the authors did not experimentally evidence fluid superheating (no temperature was measured), and they did not benefit from the plasmonic resonance of metal nanoparticles.

In 2015, Kwon and coworkers[33] reported on the photothermal-induced formation of metal-oxide (CuO and ZnO) structures in aqueous precursor solution. Here, again the temperature was not monitored and the authors did not benefit from the use of plasmonic nanoparticles. Moreover, the authors did not manage to produce crystalline structures, presumably because of the aforementioned issue, which occurs when the reactant concentration is too high or the heating duration is too long.

CONCLUSIONS

In summary, we report on an experimental technique suited to conduct solvothermal synthesis at ambient pressure, on a small scale, using plasmonic nanoparticles acting as light absorbers and nanosources of heat. We illustrate the principle with the synthesis of $In(OH)_3$ microcrystals at 200 °C in liquid water. To evidence the similarities and the differences compared with common high-pressure experiments, the effects of several parameters have been investigated: the reactant concentration, the magnitude of the temperature increase, the heating duration, and the size of the heated area. Several singular effects have been evidenced. (1) The smaller the heated region, the faster the reaction, because of an Ostwald flooding effect. Although an autoclave approach usually implies heating times longer than 20 h, one can achieve crystal formation within a few minutes using PASC. (2) A long enough heating duration leads to another type of structure (pine trees). (3) Reproducing the exact same conditions of temperature, concentration, and duration as with an autoclave approach does not lead to the formation of microcrystals. Because of too fast kinetics, we

DOI: 10.1021/acsomega.6b00019
ACS Omega 2016, 1, 2−8

rather observe the formation of a large, smooth dome. (4) The temperature dependence on the crystal morphology can be investigated in a one-shot experiment by creating a microscale temperature gradient. (5) Solvothermal reactions that normally occur in a superheated fluid can be achieved at much lower temperatures within a reasonable amount of time because of much faster kinetics. (6) Microcrystal products do not act as nucleation points for bubble formation and do not prevent the fluid from superheating. (7) Microcrystal products remain located at the substrate/solvent interface and do not diffuse in the surrounding solvent. (8) The presence of thermal-induced microscale fluid convection does not affect the crystal growth.

This work gives the guidelines for efficient solvothermal chemistry at the microscale at ambient pressure and could pave the way for new approaches suited for fundamental research on solvothermal synthesis or for practical applications in microscale patterning of nanostructures. More sophisticated PASC approaches could further benefit from the natural catalytic effect of gold nanoparticles.

■ AUTHOR INFORMATION

Corresponding Authors

*E-mail: hadrien.robert@fresnel.fr (H.R.).
*E-mail: guillaume.baffou@fresnel.fr (G.B.).

Notes

The authors declare the following competing financial interest(s): HR has been a PhD student from April 2015 with financial support that came partly from the Phasics SA company.

■ ACKNOWLEDGMENTS

This work was partly supported by the Agence Nationale de la Recherche (Grant NATO, ANR-13-BS10-0013-03). J.P. and F.K. thank Prof. R. Fässler and the Max Plank society, which financially supported this work. R.Q. and E.B.-U. acknowledge financial support from the European Community's Seventh Framework Program under grant ERC-Plasmolight (259196), the Spanish Ministry of Economy and Competitiveness, through the 'Severo Ochoa' Programme for Centres of Excellence in R&D (SEV-2015-0522) and Fundació CELLEX Barcelona. E.B.-U. acknowledges the support of the FPI fellowship from the Spanish Ministry of Science and Innovation (MICINN).

■ REFERENCES

(1) Baffou, G.; Quidant, R. Nanoplasmonics for Chemistry. *Chem. Soc. Rev.* **2014**, *43*, 3898−3907.
(2) Kale, M. J.; Avanesian, T.; Christopher, P. Direct Photocatalysis by Plasmonic Nanostructures. *ACS Catal.* **2014**, *4*, 116−128.
(3) Zhang, X.; Chen, Y. L.; Liu, R. S.; Tsai, D. P. Plasmonic Photocatalysis. *Rep. Prog. Phys.* **2013**, *76*, 046401.
(4) Wang, C.; Astruc, D. Nanogold plasmonic photocatalysis for organic synthesis and clean energy conversion. *Chem. Soc. Rev.* **2014**, *43*, 7188.
(5) Qiu, J.; Wei, W. D. Surface Plasmon-Mediated Photothermal Chemistry. *J. Phys. Chem. C* **2014**, *118*, 20735−20749.
(6) Adleman, J. R.; Boyd, D. A.; Goodwin, D. G.; Psaltis, D. Heterogenous Catalysis Mediated by Plasmon Heating. *Nano Lett.* **2009**, *9*, 4417−4423.
(7) Fasciani, C.; Alejo, C. J. B.; Grenier, M.; Netto-Ferreira, J. C.; Scaiano, J. C. High-Temperature Organic Reactions at Room Temperature Using Plasmon Excitation: Decomposition of Dicumyl Peroxide. *Org. Lett.* **2011**, *2*, 204−207.
(8) Vásquez-Vásquez, C.; Vaz, B.; Giannini, V.; Pérez-Lorenzo, M.; Alvarez-Puebla, R. A.; Correa-Duarte, M. A. Nanoreactors for Simultaneous Remote Thermal Activation and Optical Monitoring of Chemical Reactions. *J. Am. Chem. Soc.* **2013**, *135*, 13616−13619.
(9) Yen, C. W.; El-Sayed, M. A. Plasmonic Field Effect on the Hexacyanoferrate(III)-Thiosulfate Electron Transfer Catalytic Reaction on Gold Nanoparticles: Electromagnetic or Thermal? *J. Phys. Chem. C* **2009**, *113*, 19585−19590.
(10) Hung, W. H.; Aykol, M.; Valley, D.; Hou, W.; Cronin, S. B. Plasmon Resonant Enhancement of Carbon Monoxide Catalysis. *Nano Lett.* **2010**, *10*, 1314−1318.
(11) Lee, J.; Mubeen, S.; Li, X.; Stucky, G. D.; Moskovits, M. Plasmonic Photoanodes for Solar Water Splitting with Visible Light. *Nano Lett.* **2012**, *12*, 5014−5019.
(12) Warren, S. C.; Thimsen, E. Plasmonic Solar Water Splitting. *Energy Environ. Sci.* **2012**, *5*, 5133.
(13) Brongersma, M. L.; Halas, N. J.; Nordlander, P. Plasmon-Induced Hot Carrier Science and Technology. *Nat. Nanotechnol.* **2015**, *10*, 25−34.
(14) Feng, S.; Xu, R. New Materials in Hydrothermal Synthesis. *Acc. Chem. Res.* **2001**, *34*, 239−247.
(15) Baffou, G.; Polleux, J.; Rigneault, H.; Monneret, S. Super-Heating and Micro-Bubble Generation around Plasmonic Nanoparticles under cw Illumination. *J. Phys. Chem. C* **2014**, *118*, 4890.
(16) Baffou, G.; Quidant, R. Thermo-Plasmonics: Using Metallic Nanostructures as Nano-Sources of Heat. *Laser Photonics Rev.* **2013**, *7*, 171−187.
(17) Kundrat, F.; Baffou, G.; Polleux, J. Shaping and Patterning Gold Nanoparticles via Micelle Templated Photochemistry. *Nanoscale* **2015**, *7*, 15814−15821.
(18) Baffou, G.; Bon, P.; Savatier, J.; Polleux, J.; Zhu, M.; Merlin, M.; Rigneault, H.; Monneret, S. Thermal Imaging of Nanostructures by Quantitative Optical Phase Analysis. *ACS Nano* **2012**, *6*, 2452−2458.
(19) Zhu, H.; Yao, K.; Wo, Y.; Wang, N.; Wang, L. Hydrothermal synthesis of single crystalline $In(OH)_3$ nanorods and their characterization. *Semicond. Sci. Technol.* **2004**, *19*, 1020−1023.
(20) Donner, J.; Baffou, G.; McCloskey, D.; Quidant, R. Plasmon-Assisted Optofluidics. *ACS Nano* **2011**, *5*, 5457−5462.
(21) Würger, A. Thermal Non-Equilibrium Transport in Colloids. *Rep. Prog. Phys.* **2010**, *73*, 126601.
(22) Iacopini, S.; Piazza, R. Thermophoresis in Protein Solutions. *Europhys. Lett.* **2003**, *63*, 247−253.
(23) Duhr, S.; Braun, D. Why Molecules Move along a Temperature Gradient. *Proc. Natl. Acad. Sci. U.S.A.* **2006**, *103*, 19678.
(24) Tang, S.; Zhang, J.; Wu, S.; Hu, C.; Li, Y.; Jiang, L.; Cui, Q. Effects of Heating Rate on the Nucleation, Growth, and Transformation of InOOH and In_2O_3 via Solvothermal Reactions. *J. Phys. Chem. C* **2014**, *118*, 21170−21176.
(25) Guyon, E.; Hulin, J. P.; Petit, L.; Mitescu, C. D. *Physical Hydrodynamics*; Oxford University Press: USA, 2001.
(26) Yeo, J.; Hong, S.; Wanit, M.; Kang, H. W.; Lee, D.; Grigoropoulos, C. P.; Sung, H. J.; Ko, S. H. Rapid, One-Step, Digital Selective Growth of ZnO Nanowires on 3D Structures Using Laser Induced Hydrothermal Growth. *Adv. Funct. Mater.* **2013**, *23*, 3316−3323.
(27) Boyd, D. A.; Greengard, L.; Brongersma, M.; El-Naggar, M. Y.; Goodwin, D. G. Plasmon-Assisted Chemical Vapor Deposition. *Nano Lett.* **2006**, *6*, 2592−2597.
(28) Cao, L.; Barsic, D. N.; Guichard, A. R.; Brongersma, M. L. Plasmon-Assisted Local Temperature Control to Pattern Individual Semiconductor Nanowires and Carbon Nanotubes. *Nano Lett.* **2007**, *7*, 3523−3527.
(29) Hwang, D. J.; Ryu, S. G.; Grigoropoulos, C. P. Multi-Parametric Growth of Silicon Nanowires in a Single Platform by Laser-Induced Localized Heat Sources. *Nanotechnology* **2011**, *22*, 385303.
(30) Hung, W. H.; Hsu, I. K.; Bushmaker, A.; Kumar, R.; Theiss, J.; Cronin, S. B. Laser Directed Growth of Carbon-Based Nanostructures by Plasmon Resonant Chemical Vapor Deposition. *Nano Lett.* **2008**, *8*, 3278−3282.

DOI: 10.1021/acsomega.6b00019
ACS Omega 2016, 1, 2−8

(31) Haruta, M.; Kobayashi, T.; Sano, H.; Yamada, N. Novel Gold Catalysts for the Oxidation of Carbon Monoxide at a Temperature Far below 0 °C. *Chem. Lett.* **1987**, *16*, 405−408.
(32) Cho, A. Connecting the Dots to Custom Catalysts. *Science* **2003**, *299*, 1684−1685.
(33) Kwon, K.; Shim, J.; Lee, J. O.; Choi, K.; Yu, K. Localized Laser-Based Photohydrothermal Synthesis of Functionalized Metal-Oxides. *Adv. Funct. Mater.* **2015**, *25*, 2222−2229.

DOI: 10.1021/acsomega.6b00019
ACS Omega 2016, 1, 2−8